Rapid Detection of Higher Modes

Chance Jackson,[1] Kya Schluterman,[2] and Marek Szczepanczyk[3]
[1] *University of Florida*
[2] *Embry-Riddle Aeronautical University*
[3] *University of Warsaw*
(Dated: 2 August 2024)

We present a novel technique for the detection of higher modes within the gravitational wave signal, requiring only parameters derived from the coherent WaveBurst algorithm. This method relies only on leading order approximations of the frequency evolution of the signal, as well as approximations for the evolution of the higher modes. It is applied to two distinct distributions forming a statistical background and foreground for the test of the null hypothesis: that a typical signal does not contain higher mode presence. Each of these distributions is passed through noise curves for LIGO observing runs 3,4, and 5, showing how the method will improve as the sensitivity of LIGO reaches closer to its design specifications. Finally, we present the future of the method to come, outlining its current development as a part of the cWB search pipeline as well as future routes of research regarding its use.

I. INTRODUCTION

Since the first detection of gravitational waves by LIGO in 2015 (Ref. [1]), the sensitivity of ground based detectors has increased dramatically. As LIGO nears its design sensitivity with the planned A+ upgrade, an unprecedented number of compact binary systems are expected to be observed (Ref. [2]). Given this outlook, a heightened importance has been placed on rapid parameter estimation techniques, as passing every event through the computationally expensive process of matched filtering has become untenable.

Two observations during observing run 3 (O3) show unequivocal evidence of the presence of higher order multipoles: GW190814 (Ref. [3]), and GW190412 (Ref. [4]). These events were of great significance for the fields of gravitational wave data analysis and theory, as the observation of higher modes within the gravitational signal provides an orthogonal information set to the typical quadrupole mode. This creates the perfect laboratory for tests of General Relativity within the strong-field regime of the extreme binaries which produce significant higher mode amplitude. Particularly, Ref. [5]. outlines the use of higher harmonics as a method for testing the No-Hair Theorem, which posits that a black hole is completely defined by the parameters which enter the Kerr metric (charge, angular momentum, mass), relying on the differing ringdown frequencies and damping factors of the higher multipoles.

Beyond tests of General Relativity, the resolution of higher modes allows for the source parameters of the generating system to be reconstructed more accurately than is possible with the quadrupole mode only, and it allows for the breaking of degeneracies which arise within parameter estimation. For instance, a degeneracy which exists between the luminosity distance and orbital inclination of a compact binary can be resolved by exploiting the orthogonality of the different higher modes (Ref. [6]). Increasing the accuracy of distance estimations in this way could have significant cosmological implications, as accurate source distances could be used to place further constraints on the Hubble parameter (H_0).

The work of Vedovato et al. (Ref. [7]) outlined the possibility for the detection of higher modes using only the reconstructed scalograms of the coherent WaveBurst (`cWB`) algorithm (Ref. [8]). The reliance of this method on source parameters estimated from matched filtering makes it impossible to implement within the low-latency pipeline, however. We extend this paper to a model-independent, minimal assumption approach, capable of using only cWB reconstructed parameters (chirp mass, coalescence time), to rapidly generate a detection probability for higher modes. This is possible using only the leading order Newtonian approximations for the quadrupole gravitational wave signal of two inspiraling point-like particles.

This study is ordered as follows: Section II introduces the mathematics of the gravitational wave multipole expansion, and provides an outline of the coherent WaveBurst algorithm. Section III discusses the structure of our method, introducing the functions and hyperparameters used to generate optimal fits to the different mode tracks. Section III also describes the source distributions used to test our method. Finally, Sections IV and V discusses some preliminary results achieved with this method, as well as a brief summary containing future directions for this research.

II. BACKGROUND

A. Higher Multipoles of Gravitational Radiation

Gravitational radiation from the inspiral of a compact binary system is dominantly emitted at twice the orbital frequency. However, this is not the only harmonic present in the signal. Following the Newman-Penrose formalism (Ref. [9]), a general gravitational wave signal, with strain $h = h_+ - ih_\times$, can be decomposed into an infinite series of multipoles using the spin-weighted spherical harmonics:

$$h_+ - ih_\times = \sum_{l\geq 2}^{\infty} \sum_{m=-l}^{l} h_{l,m}(t, \vec{\lambda}) Y_{l,m}^{-2}(\Theta, \Phi), \quad (1)$$

where (Θ, Φ) encode information about the angular source location, and $\vec{\lambda}$ contains all intrinsic source parameters (i.e component masses). For a typical event, the vast majority of the amplitude lies in the quadrupole, $(l, |m|) = (2, 2)$, harmonic. However, events which exhibit significant asymmetry can have energy present in the subdominant harmonics. Specifically, for events with highly asymmetric component masses, a non-negligible amount of energy is expected to be present in the $(l, |m|) = (3, 3)$ harmonic (Ref. [10]).

B. Coherent WaveBurst

Coherent WaveBurst is a coherent energy detection method, developed to detect transient burst signals within the highly complex noise background present in gravitational wave detectors. The main detection pipeline of cWB can be summarized as follows. First, the time-stream detector data from each detector in the network is transformed to the time-frequency domain using the wavescan transform described in Ref. [11]. The resulting scalograms from each detector are combined, with the coherent energy between them maximized to account for any time-of-flight offsets. Given the non-stationary noise present in gravitational wave detectors, the maximization of coherent energy will cause the noise background to interfere destructively, but any signal present to interfere constructively. Finally, estimates for the gravitational wave signal are generated by applying the constrained likelihood function (Ref. [8]).

Post-detection,the cWB pipeline allows for the reconstruction of several important source parameters. Principal to our analysis, cWB is able to reconstruct the chirp mass and coalescence time of a binary within seconds of a detection. The details of the procedure for the chirp mass estimation are outlined in Ref. [12].

III. METHODS

In the leading order Newtonian approximation, the frequency evolution of the quadrupolar mode of two inspiraling point masses is governed by the equation:

$$f_{(2,|2|)}(t) = \frac{1}{\pi} \left(\frac{5}{256} \frac{1}{t_{\text{coal}} - t} \right)^{3/8} \left(\frac{GM_c}{c^3} \right)^{-5/8} \quad (2)$$

With M_c referring to the chirp mass of the binary, t_{coal} the time of coalescence, and G, c the gravitational constant and speed of light respectively (Ref. [13]). It's worth noting that, since this equation is defined for the case of two point masses, it's only valid for the inspiral phase of the waveform. Additionally, the frequency evolution of subsequent multipoles, as shown in Ref. [7], can be approximated using the relation:

$$f_{l,m}(t) \approx \frac{m}{2} f_{(2,|2|)}(t). \quad (3)$$

cWB is capable of producing rapid estimates for the chirp mass and t_{coal}. These estimated parameters gives us an initial guess for the frequency evolution of the $(2, |2|)$ and $(3, |3|)$ modes according to the above equations.

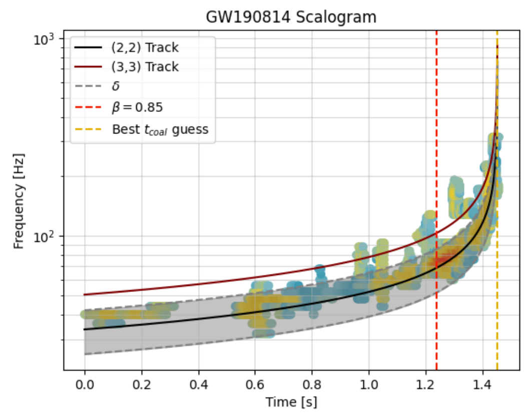

FIG. 1. Scalogram of GW190814 with the model hyperparameters defined. The tracks shown in maroon and black represent determined best fit to the $(2, |2|)$ and $(3, |3|)$ tracks, using the maximum energy approach. Bounding the $(2, |2|)$ track, the δ bandwidth shaded in grey shows the area within which pixel energy was summed. The dashed red line shows the used β cutoff, meaning only 85% of the entire signal duration was used in the calculation of the energy ratio.

Our method relies on calculating the energy around a projected path, so we say the difference between the $(2, |2|)$ and $(3, |3|)$ tracks is our bandwidth such that we cannot count pixel energy for both tracks. We also impose a so called β time cutoff factor as an upper limit time for the sake of energy summation. For the case of our calculations, we say the reconstructed t_{coal} corresponds to $\beta = 1$ and $\beta = 0$ is the start time for the signal. This β cutoff ensures we don't count energy in the merger phase, as this is where contributions from each mode overlaps and the simple frequency evolution defined in Eq. 2 breaks down. In order to ensure our projected $(2, |2|)$ track lay on the path with the most energy, we allow a fitting parameter α to scale the track frequency. We expect the $(2, |2|)$ track to appear near $\alpha = 1$ and the $(3, |3|)$ track to appear at $\frac{3}{2}$ times the $(2, |2|)$ frequencies according to Eq. 3. We also fit the coalescence time with an offset according to the same best-energy maximisation. We then sum all of the energy within the $(3, |3|)$ band and divide it by the $(2, |2|)$ energy, returning our energy ratio test statistic:

$$\eta = \frac{E_{(3,|3|)}}{E_{(2,|2|)}} \quad (4)$$

A. Tuning the Method

The presence of free hyper-parameters δ, β within our model necessitates tuning. We know the frequency evolution breaks down near coalescence so we can't rely on any meaningful energy ratio here. The magnitude of contribution from the $(3, |3|)$ mode is also greatest at higher frequencies, so we needed to balance the harshness of our beta threshold in order to maximize detection likelihood. For the collection of the results presented in Section IV, we follow the convention of Ref.[7] in defining δ to be equal to half the distance between the $(2, |2|)$ and $(3, |3|)$ tracks.

Preliminary testing was conducted on the impact of β on the quality of the fit and returned η, however this hyperparameter still requires significant optimization. For the duration of this study, a β value of 0.85 was selected, as it showed a good compromise in not cutting off too much of the late inspiral stage of the signal and not allowing for significant leakage from the merger phase.

B. Distributions

In order to test the efficacy of our method, several distributions of gravitational wave events were generated. The primary distribution comprised events generated from GWTC-3 data, or the population of compact binaries expected based on gathered O3 data (Ref. [14]), giving us a realistic distribution of source parameters. It's anticipated the number of events within this distribution containing significant higher mode amplitude is small, making it an ideal background distribution for application of the test statistic. A foreground distribution of events with expected higher modes was generated from the GW190814 parameter estimation distribution. This distribution comprised the highest SNR waveforms from the matched filtering analysis of GW190814. These two distributions formed the bulk of our analysis, and representative plots of the parameter space of each are shown in Fig. 2. The background of realistic events and foreground of higher mode events were separately passed through the cWB detection pipeline, with noise curves corresponding to analytical noise curves for O3 and O4, and a theoretical noise curve for O5.Simplified fits to these noise curves for LIGO-Hanford are shown in Fig. 3. Future work will include the extension of each of these distributions to include only waveforms which contain contribution from the $(2, |2|)$ mode. In this way, we create a perfect background to compare against, allowing us to determine how often our test returns false-positives.

IV. RESULTS

Unfortunately, the results presented in this section are preliminary. Through the application of the method to each of the distributions outlined previously, we obtained

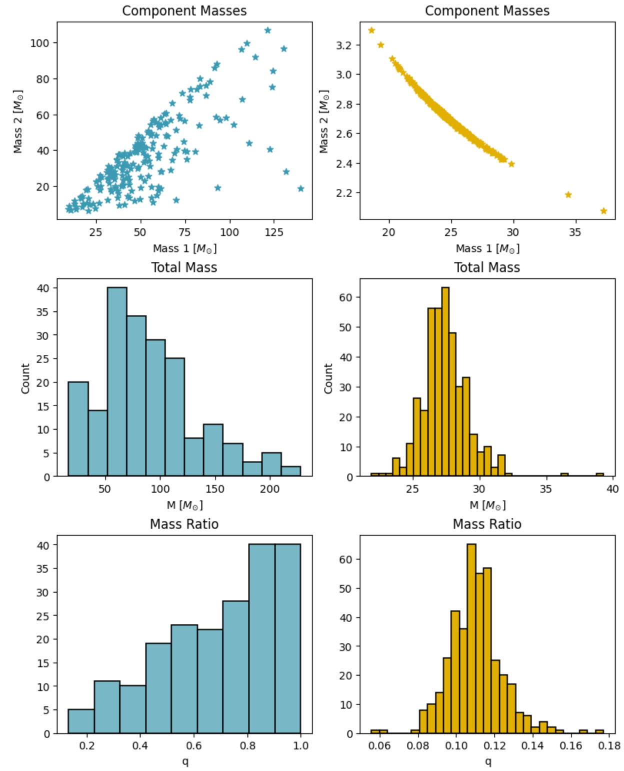

FIG. 2. Parameter space studied in each distribution used. The left column corresponds to the distribution derived from GWTC-3, representing a more realistic collection of events. The right column comes from the highest SNR matched filtering waveforms for GW190814. These two distributions formed the background (few events with $(3, |3|)$) and foreground (many events with $(3, |3|)$) for the application of our test statistic. For clarity, the top plot of each column shows a scatterplot of the component masses of the binary, whie the lower histograms show the distribution of total mass, M, and mass ratio, q, present in the distribution.

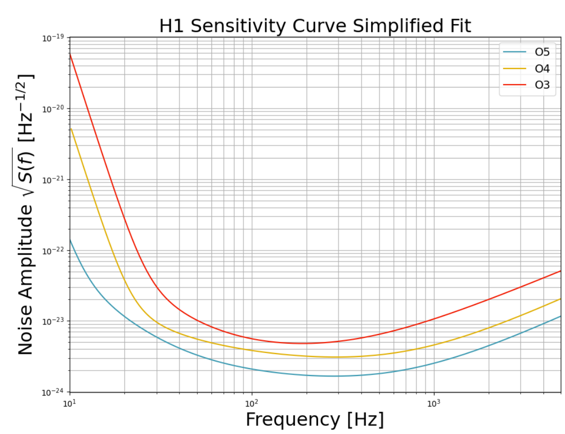

FIG. 3. Simplified fit to analytical LIGO-Hanford sensitivity curves during observing runs 3 and 4, as well as the predicted sensitivity curve for observing run 5.

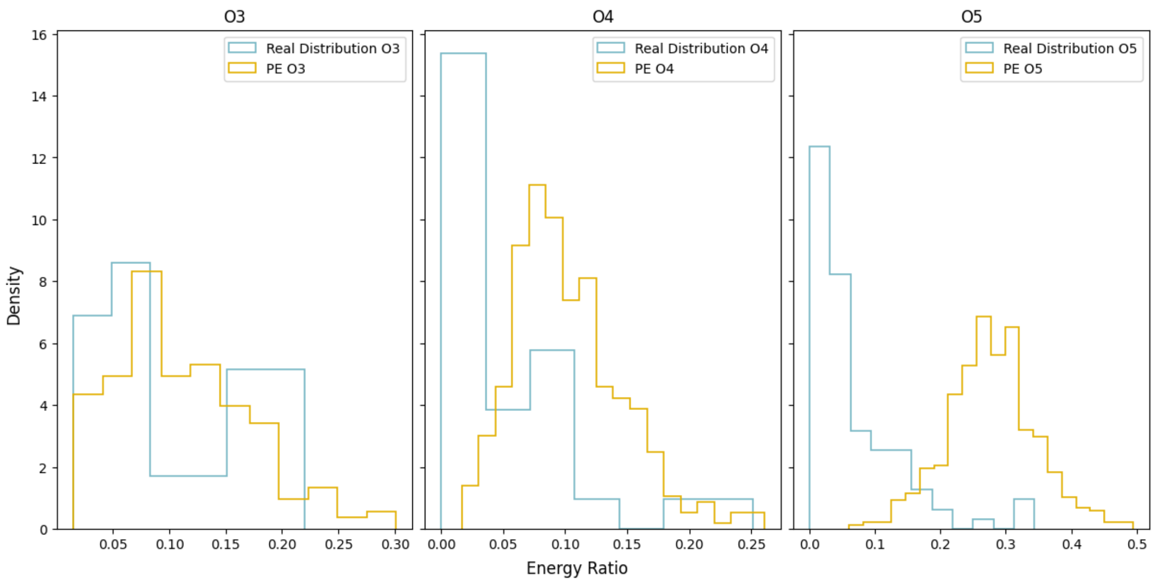

FIG. 4. Energy ratio histograms for each distribution passed through each LIGO noise curve. We see a clear separation between the background and foreground distributions by O5, showing our method to be effective in differentiating between signals with and without higher mode presence.

the histograms of Fig. 4. This was the principal result achieved, but it shows that our method is able to consistently distinguish between a signal with signficant higher mode presence (given by the parameter estimation distribution) and the background of signals which do not. We also see that even with the sensitivity of O4, we are able to differentiate background signals with no higher mode presence from signals with strong higher mode presence. Moving into the O5 noise curve, this fact becomes even more present.

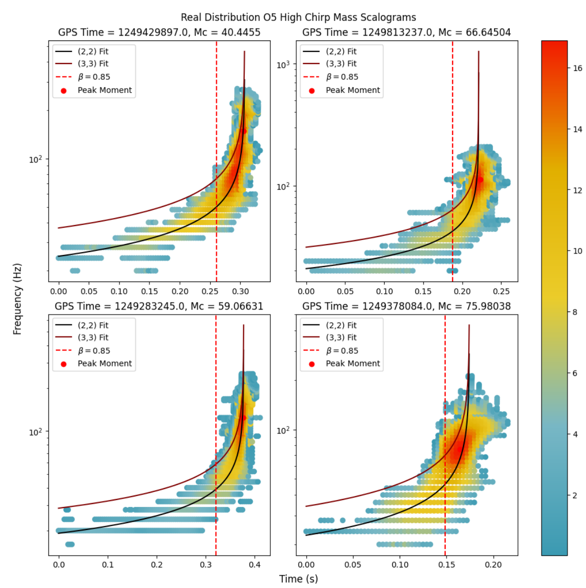

FIG. 5. High chirp mass signals from the realistic distribution, passed through the noise curve of LIGO O5.

A. Limitations

Several limitations regarding the implementation of the method outlined here presented themselves during the course of our study. Principally, strict SNR and chirp mass cutoffs were required to ensure the signal being fit to had a strong chirping structure. The SNR cutoff is intuitive, if a signal is not strong enough we will not be able to properly fit to it, but the chirp mass cutoff is slightly more subtle.

It was discovered that high chirp mass signals have a tendency to have their energy "smeared" across a broad range of frequencies at any given time. This makes it quite difficult to generate accurate estimates for the energy ratio, as energy from the $(2,|2|)$ can begin to leak into the region under the $(3,|3|)$ track. Likely, this smearing effect is a combination of multiple factors. First, the wavelet transform of cWB can suffer from spectral leakage, becoming particularly problematic for the louder signals generated by high chirp binaries. Second, the amount of time high chirp signals spend within the LIGO band is shorter than that of low chirp signals, and the portions of the high chirp signal which enter the LIGO band are much closer to the merger. Figure 7 shows this effect, higher chirp signals have much shorter durations. Figures 5 and 6 show example signals from the realistic distribution with high and low chirp masses respectively. The smearing effect is evident in the structure of these signals. To limit the impact of this effect on our estimator, only signals with a chirp mass below 40 solar masses

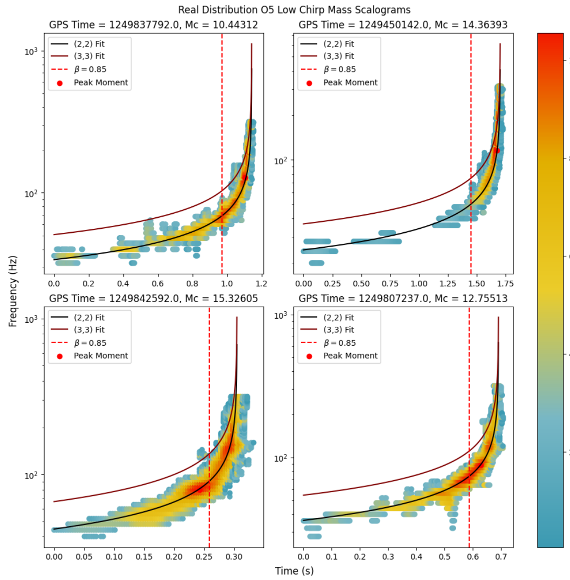

FIG. 6. Low chirp mass signals from the realistic distribution, passed through the noise curve of LIGO O5.

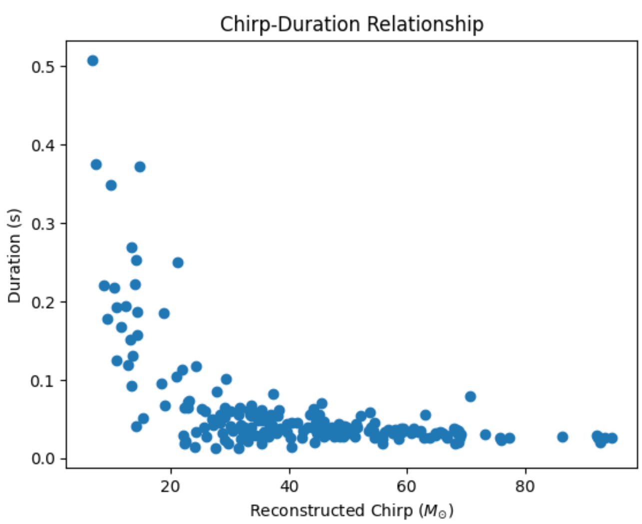

FIG. 7. Relationship between reconstructed chirp and signal duration for the realistic distribution passed through the projected LIGO noise curve for O5.

were considered.

V. SUMMARY

Over the course of this project, we were able to develop a novel method for the rapid detection of signals with higher order modes. This tool is able to consistently differentiate between a background distribution with little to no presence of higher modes and a foreground distribution which contains strong higher modes. Already, development has begun on the implementation of this tool within the cWB pipeline, and it's expected to begin use in LIGO O4.

A. Future Work

Though our tool is already being developed for implementation into cWB, a large amount of optimization work remains. A gap is present in the definition of our background and foreground distributions, in that our background distribution still contains some signals with likely presence of higher modes due to their extreme mass ratios. To combat this, distributions will be created in the future comprised of only waveforms with contributions from the $(2, |2|)$ mode, generated artificially based on the parameters of the realistic and parameter estimation distributions described previously. This should represent a more ideal background distribution, allowing for more rigorous tests of the null hypothesis: that a typical detected signal does not contain significant higher mode presence. Additionally, as the model relies on several hyperparameters, a more in-depth analysis of the optimal hyperparameters must be conducted.

B. Acknowledgments

Chance Jackson would like to thank his collaborator, Kya Schluterman, and advisor, Marek Szczepanczyk. He'd also like to thank the organizers: Paul Fulda, Peter Wass, and Sujata Krishna, and the NSF for their contribution in making this summer research possible. Finally, Chance and Kya would like to thank Gabriel Lourenço, Maciej Kierkla, Mateusz Zych, Piotr Toczek, and all the other people who made their time in Poland as great as it was.

[1] B. P. Abbott, R. Abbott, T. D. Abbott, M. R. Abernathy, F. Acernese, K. Ackley, C. Adams, T. Adams, P. Addesso, R. X. Adhikari, et al. (LIGO Scientific Collaboration and Virgo Collaboration), Phys. Rev. Lett. **116**, 061102 (2016), URL https://link.aps.org/doi/10.1103/PhysRevLett.116.061102.

[2] B. P. Abbott, R. Abbott, T. D. Abbott, S. Abraham, F. Acernese, K. Ackley, C. Adams, V. B. Adya, C. Affeldt, M. Agathos, et al., Living Reviews in Relativity **23** (2020), ISSN 1433-8351, URL http://dx.doi.org/10.1007/s41114-020-00026-9.

[3] R. Abbott, T. D. Abbott, S. Abraham, F. Acernese, K. Ackley, C. Adams, R. X. Adhikari, V. B. Adya, C. Affeldt, M. Agathos, et al., The Astrophysical Journal Letters **896**, L44 (2020), ISSN 2041-8213, URL http://dx.doi.org/10.3847/2041-8213/ab960f.

[4] R. Abbott, T. Abbott, S. Abraham, F. Acernese, K. Ackley, C. Adams, R. Adhikari, V. Adya, C. Affeldt, M. Agathos, et al., Physical Review D **102** (2020), ISSN 2470-0029, URL http://dx.doi.org/10.1103/PhysRevD.102.043015.

[5] I. Ota and C. Chirenti, Physical Review D **101** (2020), ISSN 2470-0029, URL http://dx.doi.org/10.1103/PhysRevD.101.104005.

[6] Y. Gong, Z. Cao, J. Zhao, and L. Shao, *Including higher harmonics in gravitational-wave parameter estimation and cosmological implications for lisa* (2023), 2308.13690, URL https://arxiv.org/abs/2308.13690.

[7] G. Vedovato, E. Milotti, G. A. Prodi, S. Bini, M. Drago, V. Gayathri, O. Halim, C. Lazzaro, D. Lopez, A. Miani, et al., Classical and Quantum Gravity **39**, 045001 (2022), ISSN 1361-6382, URL http://dx.doi.org/10.1088/1361-6382/ac45da.

[8] S. Klimenko et al., Phys. Rev. D. **93**, 042004 (2016).

[9] K. S. Thorne, Rev. Mod. Phys. **52**, 299 (1980), URL https://link.aps.org/doi/10.1103/RevModPhys.52.299.

[10] C. Mills and S. Fairhurst, Physical Review D **103** (2021), ISSN 2470-0029, URL http://dx.doi.org/10.1103/PhysRevD.103.024042.

[11] S. Klimenko, *Wavescan: multiresolution regression of gravitational-wave data* (2022), 2201.01096, URL https://arxiv.org/abs/2201.01096.

[12] V. Tiwari, S. Klimenko, V. Necula, and G. Mitselmakher, Classical and Quantum Gravity **33**, 01LT01 (2015), ISSN 1361-6382, URL http://dx.doi.org/10.1088/0264-9381/33/1/01LT01.

[13] M. Maggiore, *Gravitational Waves. Vol. 1: Theory and Experiments* (Oxford University Press, 2007), ISBN 978-0-19-171766-6, 978-0-19-852074-0.

[14] T. L. S. Collaboration, the Virgo Collaboration, the KAGRA Collaboration, R. Abbott, T. D. Abbott, F. Acernese, K. Ackley, C. Adams, N. Adhikari, R. X. Adhikari, et al., *The population of merging compact binaries inferred using gravitational waves through gwtc-3* (2022), 2111.03634, URL https://arxiv.org/abs/2111.03634.